Available online at www.sciencedirect.com
SCIENCE DIRECT
Polymer 46 (2005) 10085–10091
polymer
www.elsevier.com/locate/polymer

Fully exfoliated nanocomposite from polypyrrole graft copolymer/clay

Woo Jin Bae[a], Keon Hyeong Kim[a], Won Ho Jo[a,*], Yun Heum Park[b]

[a]*Hyperstructured Organic Materials Research Center and School of Materials Science and Engineering, Seoul National University, Seoul 151-742, South Korea*
[b]*School of Applied Chemistry and Chemical Engineering, Sungkyunkwan University, Suwon 440-746, South Korea*

Received 26 January 2005; received in revised form 29 June 2005; accepted 31 July 2005
Available online 15 August 2005

Abstract

Exfoliated polypyrrole graft copolymer/clay nanocomposites were prepared by in situ polymerization of pyrrole onto pre-exfoliated water-soluble poly(styrenesulfonic acid-*co*-pyrrolylmethyl styrene) (P(SSA-*co*-PMS))/clay nanocomposite or by simple blending of poly(styrenesulfonic acid-*g*-pyrrole) (PSSA-*g*-PPY) with clay. As the clay content in PSSA-*g*-PPY/clay nanocomposite increases, the conductivity of PSSA-*g*-PPY/clay nanocomposite decreases. Thermal de-doping temperature shifts to higher temperature as the clay content in PSSA-*g*-PPY/clay nanocomposite increases.

Keywords: Polypyrrole; Clay; Nanocomposite

1. Introduction

Interest in the development of new inorganic/organic nanocomposites has grown in recent years due to a wide range of potential use of these materials [1–3]. These hybrids constitute a class of advanced composite materials with unusual properties, which can be used in many fields such as optics, ionics, electronics, and mechanics.

Conducting polymers have become a popular basic material for advanced applications such as electrode [4], static electricity dissipation [5], metal anti-corrosion and marine-fouling prevention [6,7]. As one of the novel conducting polymers, polypyrrole (PPY) has been widely studied due to its good thermal and environmental stability as well as its superior electric conductivity [8,9], and electrorheological properties [10]. However, the physical properties and solubility of PPY are not satisfactory for practical applications. In this regard, PPY/clay nanocomposite may open a way to construct a novel organic–inorganic hybrid system showing electrical conductivity as well as good physical properties [11–13].

There are two main synthetic methods to obtain PPY/clay nanocomposites. One is the intercalation of a monomer followed by subsequent chemical in situ polymerization [14–16]. The other method is the direct intercalation of PPY chains into the gallery between silicate layers from solution [17,18]. In this method, water-soluble or colloidal PPY should be first prepared for its penetration into the gallery of silicate layers. Emulsion polymerization is also used for preparation of PPY/clay nanocomposite, where the emulsifier in polymerization system contributes to maximizing the affinity between hydrophilic host (clay) and hydrophobic guest (pyrrole) [19–21].

Although many studies on PPY/clay nanocomposites have been reported as mentioned above, most of results have obtained the intercalative structure. Since the exfoliated nanocomposite has better physical properties such as stiffness, strength, and barrier property with far less inorganic content than the intercalative nanocomposite, it is rationalized that the higher the degree of exfoliation in polymer/clay nanocomposites, the greater the enhancement of these properties [22].

Recently we successfully synthesized a water-soluble and self-doped conducting PPY graft copolymer, poly(-styrene sulfonic acid-*g*-pyrrole) (PSSA-*g*-PPY) [23]. Owing to its water solubility, it is likely expected that the graft copolymer could be homogeneously mixed with silicate

* Corresponding author. Tel.: +82 2 880 7192; fax: +82 2 885 1748.
E-mail address: whjpoly@plaza.snu.ac.kr (W.H. Jo).

0032-3861/$ - see front matter © 2005 Elsevier Ltd. All rights reserved.
doi:10.1016/j.polymer.2005.07.102

layers dispersed in water, and as a result the PPY/clay nanocomposite with exfoliated structure could be prepared.

In this study, we report that an exfoliated polypyrrole graft copolymer (PSSA-*g*-PPY)/clay (Na^+-MMT) nanocomposite without organophilic modification of Na^+-MMT is first prepared by using both in situ polymerization and simple blending of water-soluble PSSA-*g*-PPY with Na^+-MMT. We also report the effect of the clay content on thermal and electrical properties of the exfoliated nanocomposite.

2. Experimental

2.1. Preparation of in situ PSSA-g-PPY/clay nanocomposite

All the chemicals used in this study were purchased from Sigma-Aldrich. For synthesis of pyrrolylmethyl styrene (PMS), potassium pyrrole salt was first synthesized by reaction of pyrrole (1 ml) with potassium hydride (2 g) for 6 h at room temperature under N_2 in 100 ml of tetrahydrofuran (THF). After the temperature was lowered to 0 °C in water/ice bath, chloromethyl stryrene (CMS) (3 g) was added to the solution and the solution was stirred at 0 °C for 12 h. The organic phase was then separated and washed with water several times. Finally, the solvent was evaporated under reduced pressure. The crude product was purified by column chromatography on silica gel eluting with *n*-hexane ($R_f = 0.1$) to yield PMS as a yellow liquid (yield 68%).

Poly(sodium styrenesulfonate-*co*-pyrrolylmethyl styrene) (P(SSNa-*co*-PMS)) was synthesized by copolymerization of SSNa and PMS using 2,2′-azobisisobutyronitrile (AIBN) as an initiator. SSNa (10 g), PMS (1 ml), and AIBN (0.1 g) are dissolved in 120 ml of di-methylsulfoxide (DMSO) and then polymerized at 90 °C for 36 h under N_2 atmosphere. After polymerization, the product was precipitated into acetone, filtered, washed several times with acetone, and dried in vacuum oven at 60 °C for 24 h. The PMS content in P(SSNa-*co*-PMS) is determined ca. 7.8 mol% from the peak integration of the ^1H NMR spectrum. ^1H NMR (D_2O): $\delta = 0.8$–2.2 (broad, 3H, –C*H*$_2$–C*H*–), 5.1 (s, 2H, –Ar–C*H*$_2$–N–), 5.9 and 6.2 (s, 4H, pyrrole-*H*), 6.0–8.0 (broad, 4H, Ar–*H*). The Na^+-MMT (Closite® Na^+: Southern Clay Products Inc.; natural clay, water content < 2.0 wt%, aspect ratio = 100–1000, cation exchange capacity = 0.93 meq/g) (0.02–0.3 g) and P(SSNa-*co*-PMS) (0.8 g) were mixed in 30 ml of HCl 1 M aqueous solution and then sonicated for 3 h using an ultrasonic generator for swelling of the Na^+-MMT. The swelling procedure under an acidic condition not only helps a polymer chain to penetrate into the gallery of clay layers but also induces ion-exchange of Na^+ with H^+, which transforms from sodium sulfonate group (–SO_3Na) to sulphonic acid group (–SO_3H). For graft copolymerization of pyrrole onto poly(styrenesulfonic acid-*co*-pyrrolylmethyl styrene) (P(SSA-*co*-PMS)), pyrrole (0.1 ml) is first added to the P(SSA-*co*-PMS)/Na^+-MMT aqueous suspension for 0.5 h under stirring, and then 50 ml of ammonium persulfate (0.33 g)/HCl aqueous solution (1 M) is dropwise added at 0 °C. After 6 h of reaction, a dark suspension was obtained and then filtered. The filtered suspension was further purified by dialysis using a semipermeable membrane (molecular weight cutoff, 3500). The purified suspension was concentrated in a vacuum evaporator and then coagulated in acetone to give solid powder. The chemical structures of polymers used in this work are represented in Fig. 1. The sample codes for in situ PSSA-*g*-PPY/clay nanocomposites are listed in Table 1.

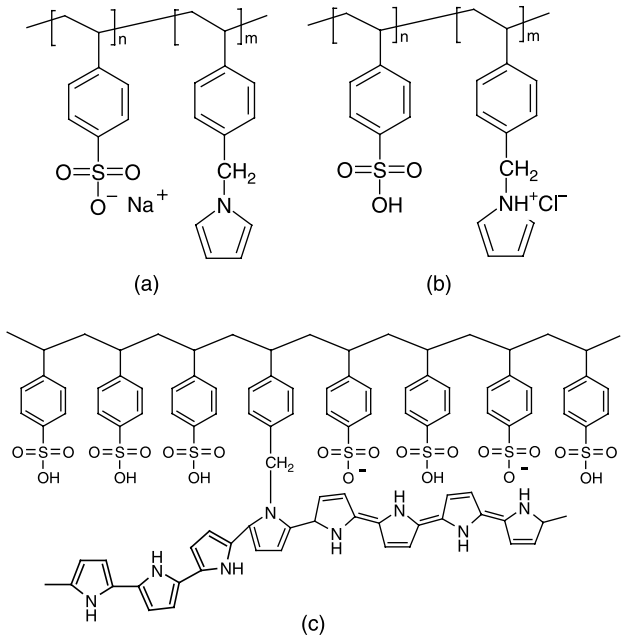

Fig. 1. Chemical structures of (a) P(SSNa-*co*-PMS); (b) P(SSA-*co*-PMS) (protonated form); (c) PSSA-*g*-PPY.

2.2. Simple blending of P(SSNa-co-PMS) and clay

Na^+-MMT (0.15 g) and P(SSNa-*co*-PMS) (1.0 g) were mixed in de-ionized water and then sonicated for 3 h using an ultrasonic generator for swelling of the Na^+-MMT. The suspension was concentrated and coagulated into acetone.

Table 1
Sample codes for in situ composites PSSA-*g*-PPY/clay

Sample code	Clay wt% in nanocomposite[a]
In situ composites of PSSA-*g*-PPY/clay	
InSituComp2	2.0
InSituComp4	3.9
InSituComp9	9.1
InSituComp13	13.0
InSituComp17	16.7
InSituComp29	28.6

[a] Measured by thermogravimetric analysis.

The coagulation was filtered and dried under vacuum at 60 °C for 24 h.

2.3. Simple blending of PSSA-g-PPY and clay

Na^+-MMT (0.15 g) and PSSA-*g*-PPY (1.0 g; the PPY content: 36 mol%; see Ref. [23]) were mixed in de-ionized water and then sonicated for 3 h using an ultrasonic generator for swelling of the Na^+-MMT. The suspension was concentrated and coagulated into acetone. The coagulation was filtered and dried under vacuum at 60 °C for 24 h.

2.4. Characterization

The change in basal spacing of silicate layers was measured using an X-ray diffractometer (MAC Science, MXP 18XHF) with Ni-filtered Cu Kα radiation (λ = 0.1542 nm; 40 kV; 30 mA) and small-angle X-ray scattering (SAXS) (Bruker, Nanostar) with monochromatized Cu Kα radiation (λ = 0.1542 nm; 40 kV; 35 mA; scattering angle ranges between 0.05 and 2.6°). Transmission electron microscope (TEM) (JEOL-200CX) was used with an acceleration voltage of 120 kV. The samples for TEM were prepared by evaporation of a drop of diluted aqueous solution of the nanocomposite onto a 200 mesh copper grid. FTIR spectra were recorded on a Perkin–Elmer FTIR 1725X spectrometer, and UV–vis–NIR spectra of PSSA-*g*-PPY/clay nanocomposite were obtained using a Perkin–Elmer UV–vis–NIR spectrophotometer (model Lambda-6). The electrical conductivity of PSSA-*g*-PPY/clay nanocomposite was measured in a compressed pellet (1.5 cm diameter × 0.05 cm thick) at room temperature by the four-probe technique using an electrometer. Details of experiment for measuring electrical conductivity were described in an earlier paper [18]. Temperature dependence of electrical conductivity was examined by measuring the conductivity at various temperatures, after the pellet was dried in vacuum at 60 °C over 24 h.

3. Results and discussion

The FTIR spectrum of P(SSNa-*co*-PMS) (Fig. 2(b)) exhibits absorption peaks characteristic of PMS at 1630, 1565 and 1397 cm^{-1}, which are absent in the spectrum of PSSNa homopolymer (Fig. 2(a)), indicating that the PMS is copolymerized with SSNa. When the FTIR spectrum of P(SSNa-*co*-PMS)/clay (simple blending in water) (Fig. 2(c)) is compared with that of P(SSNa-*co*-PMS) (Fig. 2(b)), characteristic peaks of clay (Na^+-MMT) were observed at 1078, 521, and 465 cm^{-1} in Fig. 2(c) [24,25]. When the FTIR spectrum of P(SSNa-*co*-PMS)/clay (simple blending in water) (Fig. 2(c)) is compared with that of P(SSA-*co*-PMS)/clay (simple blending in 1 M HCl aqueous solution) (Fig. 2(d)), it reveals that new absorption peaks at 1705 and 1175 cm^{-1} (ν_{N-H^+} (imine hydrohalide stretching vibration, i.e. $NH^+\cdots Cl^-$) and ν_{O-H} (observed in covalent (non-ionized) sulphonic acids), respectively) are observed in the spectrum of P(SSA-*co*-PMS)/clay (Fig. 2(d)). The P(SSA-*co*-PMS), the protonated form of P(SSNa-*co*-PMS), can interact with anionic charged surface of clay, which will be discussed later.

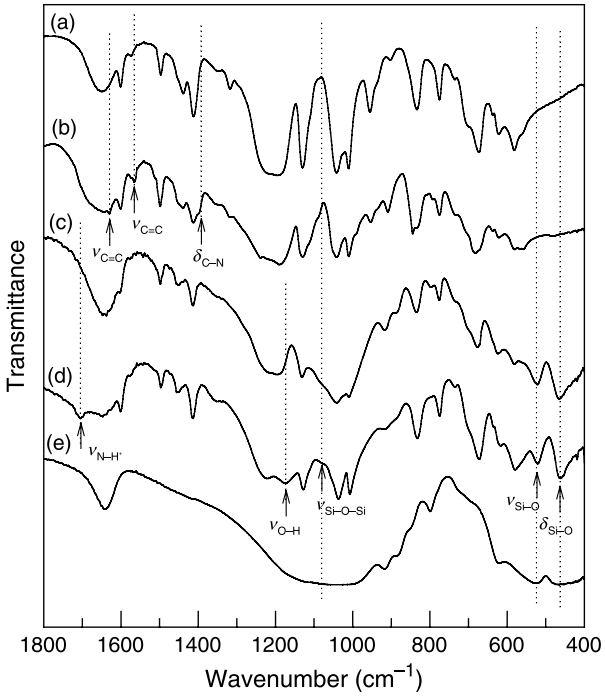

Fig. 2. FTIR spectra of (a) PSSNa; (b) P(SSNa-*co*-PMS); (c) P(SSNa-*co*-PMS)/clay (simple blending in water); (d) P(SSA-*co*-PMS)/clay (simple blending in 1 M HCl aqueous solution); (e) Na^+-MMT.

The FTIR spectrum of PSSA-*g*-PPY shows that the representative vibration bands of PPY are observed at 1548, 1450, 1404, 1325 and 896 cm^{-1}, corresponding to $\nu_{C=C}$ (in pyrrole ring), ν_{C-N}, $\nu_{C=C}$ (in pyrrole ring), δ_{C-N}, and δ_{C-H} (out-of-plane deformation) [23,26], respectively, as shown in Fig. 3, indicating that polypyrrole is successfully grafted onto P(SSA-*co*-PMS). The FTIR spectra of a series of in situ composites of PSSA-*g*-PPY and clay (InSituComp) show characteristic peaks of Na^+-MMT at 1060, 561, and 465 cm^{-1} corresponding to $\nu_{Si-O-Si}$, ν_{Si-O}, and δ_{Si-O}, respectively, [25]. As the clay content in PSSA-*g*-PPY/clay increases, the intensities of characteristic peaks of clay (1060, 561, and 465 cm^{-1}) increase.

X-ray diffraction (XRD) has often been used for determining the degree of intercalation and/or exfoliation of clay in the polymer matrix. When XRD patterns for pristine clay (Na^+-MMT), P(SSNa-*co*-PMS)/clay (simple blending in water), P(SSA-*co*-PMS)/clay (simple blending in HCl 1 M aqueous solution), and a series of InSituComp are compared with each other, as shown in Fig. 4, the following facts are realized. First, the *d*-spacing of Na^+-MMT in P(SSNa-*co*-PMS)/clay (simple blending in water) increases from 0.98 nm of pristine clay to 0.13 nm, as shown in Fig. 4(a) and (b), indicating that P(SSNa-*co*-PMS)

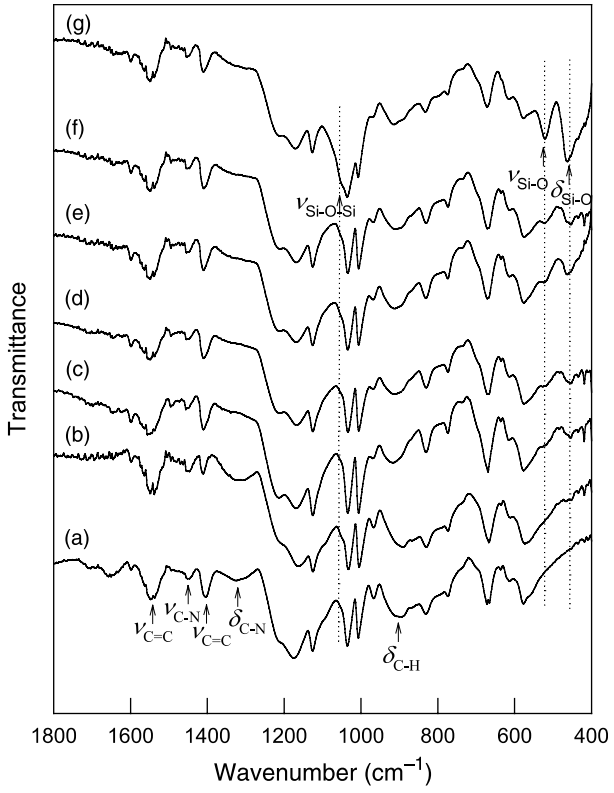

Fig. 3. FTIR spectra of (a) PSSA-*g*-PPY; (b) InSituComp2; (c) InSituComp4; (d) InSituComp9; (e) InSituComp13; (f) InSituComp17; (g) InSituComp29.

chains are intercalated into the gallery of clay layers. Secondly, P(SSA-*co*-PMS)/clay (simple blending in HCl 1 M aqueous solution) does not exhibit any discernible peak in the XRD pattern (Fig. 4(c)), indicating that most of clay layers are exfoliated in the polymer matrix. Since the P(SSA-*co*-PMS) obtained in an acidic aqueous medium has positively charged nitrogens in its structure, it is expected

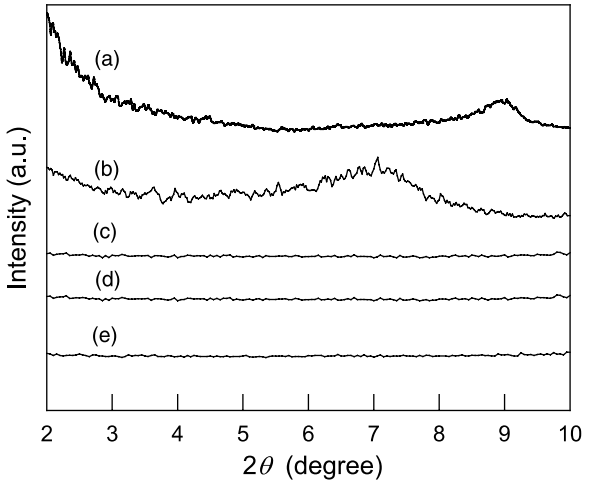

Fig. 4. XRD patterns of (a) Na^+-MMT; (b) P(SSNa-*co*-PMS)/clay (simple blending in water); (c) P(SSA-*co*-PMS)/clay (simple blending in 1 M HCl aqueous solution); (d) PSSA-*g*-PPY/clay (simple blending in water); (e) InSituComp29.

that an ionic interaction between positively charged nitrogen in P(SSA-*co*-PMS) and negatively charged surface of clay layers leads to exfoliation of clay layers in the polymer matrix. Third, the XRD pattern of InSituComp29 shows an exfoliated structure, as can be seen in Fig. 4(e). The XRD patterns of InSituComp2, 4, 9, 13 and 17 are the same as that of InSituComp29 and so not shown in Fig. 4. This indicates that the exfoliated structure of P(SSA-*co*-PMS)/clay is preserved while the composite of PSSA-*g*-PPY/clay is prepared by in situ graft copolymerization of pyrrole onto P(SSA-*co*-PMS)/clay. Here, it is noteworthy that PSSA-*g*-PPY is more favorable to interact with negatively charged surface of clay layers than the P(SSA-*co*-PMS), because PSSA-*g*-PPY has much more positive charges than does P(SSA-*co*-PMS) to interact with the negative charge of clay surface. Finally, the simple blending of water-soluble PSSA-*g*-PPY and Na^+-MMT also yields an exfoliated structure (Fig. 4(d)).

Small-angle X-ray scattering is useful for investigating a more complex multiscale, multiphase structure, while WAXS has a limit for investigation of the superstructure of layered silicate in polymer matrix [27]. Since small-angle X-ray diffraction of in situ nanocomposites below 2 theta = 2θ do not show any discernible peak, as shown in Fig. 5, it is concluded that the in situ nanocomposites have exfoliated structure of clay layers.

To more directly identify exfoliated structures of the nanocomposites, we obtained TEM images of the composites, as shown in Fig. 6, where dark stripes represent the clay layers and the gray/white area represents the polymer matrix. TEM images of InSituComp13 (Fig. 6(a)), simple blending of PSSA-*g*-PPY and clay (Fig. 6(b)), and P(SSA-*co*-PMS)/clay (simple blending in HCl 1 M aqueous solution) (Fig. 6(c)) show fully exfoliated structures, i.e., the nano-sized clay sheets are uniformly dispersed in the polymer matrix, whereas the TEM image of P(SSNa-*co*-PMS)/clay (simple blending in water) (Fig. 6(d)) shows that the composite has some amount of stacked layers in which

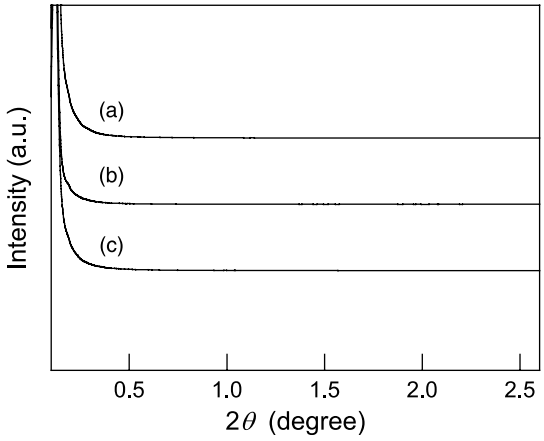

Fig. 5. SAXS patterns of (a) P(SSA-*co*-PMS)/clay (simple blending in 1 M HCl aqueous solution); (b) PSSA-*g*-PPY/clay (simple blending in water); (c) InSituComp29.

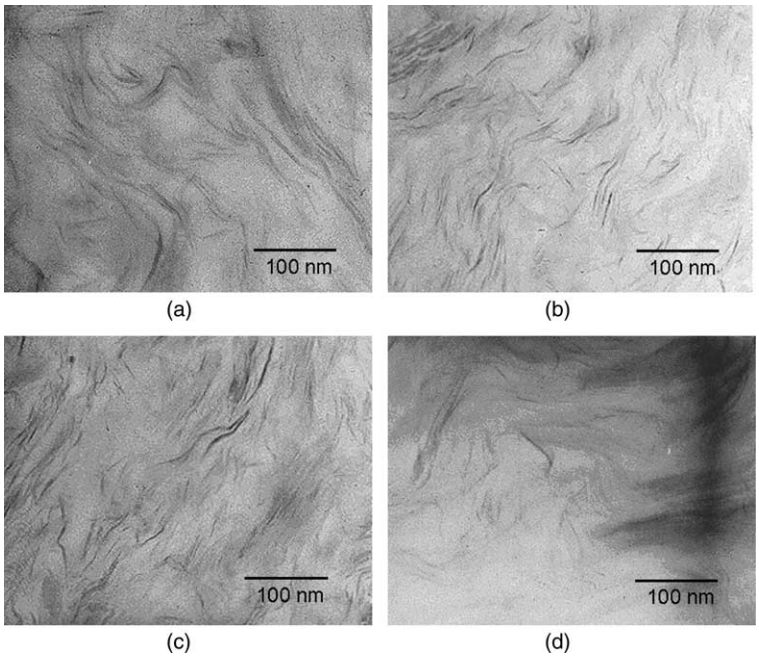

Fig. 6. TEM images of (a) InSituComp13; (b) PSSA-*g*-PPY/clay (simple blending in water); (c) P(SSA-*co*-PMS)/clay (simple blending in 1 M HCl aqueous solution); (d) P(SSNa-*co*-PMS)/clay (simple blending in water).

polymer chains are intercalated, which is consistent with the result of WAXS (Fig. 4(b)).

When the electrical conductivities of in situ nanocomposites are plotted as a function of the clay content, the logarithm of conductivity decreases linearly with the increase of clay content, as can be seen in Fig. 7. This is because the content of conducting part (PPY) in PSSA-*g*-PPY/clay nanocomposite decreases with increasing the clay content. Here, it is interesting to note that the PPY content (calculated from elemental analysis) in PSSA-*g*-PPY linearly increases with increasing the clay content added to in situ graft polymerization system, although the PPY content in in situ nanocomposite decreases, as can be seen in Fig. 8. The increase of PPY content with the clay content in the in situ nanocomposite implies that the clay plays a catalytic role during graft copolymerization of PPY. Indeed, as the clay contents increases, the initiation time for polymerization of pyrrole decreases from 1 h for PSSA-*g*-PPY to 5 min for InSituComp29. The initiation time for graft polymerization of pyrrole is identified by the color change of the solution from colorlessness to black. From the above result, it is concluded that the clay, which has anionic character, catalyzes polymerization of pyrrole (cationic character), although the detailed mechanism is not clearly identified.

The UV–vis–NIR spectra of a series of InSituComp show that all the samples have a bipolaron absorption at 465–

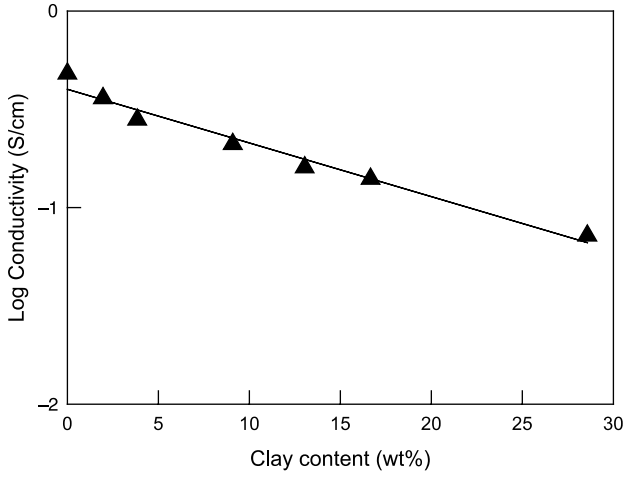

Fig. 7. Log conductivity of InSituComp plotted against the clay content.

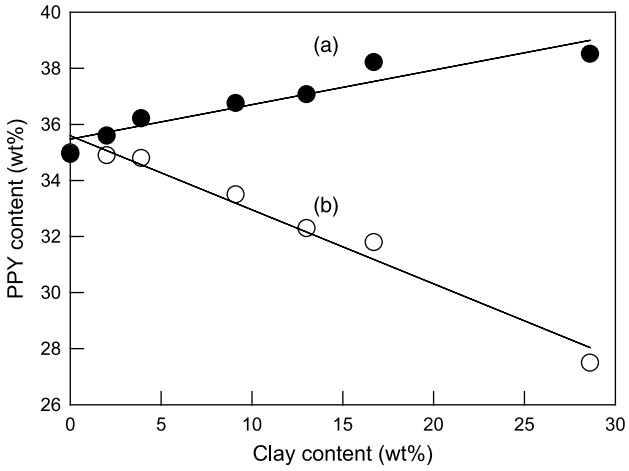

Fig. 8. The PPY content (a) in graft copolymer (PSSA-*g*-PPY) and (b) in nanocomposite (InSituComp) as a function of the clay content, when pyrrole is in situ grafted onto P(SSA-*co*-PMS)/clay.

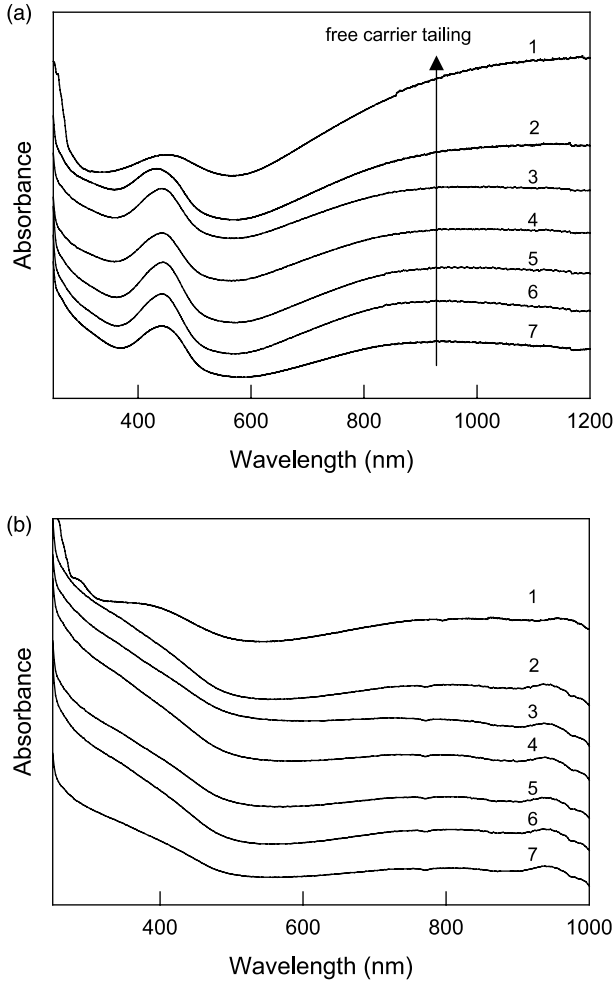

Fig. 9. UV visible spectra of (a) doped sate and (b) de-doped state of (1) PSSA-*g*-PPY; (2) InSituComp2; (3) InSituComp4; (4) InSituComp9; (5) InSituComp13; (6) InSituComp17; (7) InSituComp29.

475 nm and a free carrier tailing in the near-IR region with a maximum at above 1000 nm, as shown in Fig. 9(a), indicating that in situ nanocomposites are in a self-doped state. The intensity of free carrier tailing decreases as the clay content in in situ nanocomposites increases, which results from decreased conductivity (Fig. 7). After de-doping of in situ nanocomposites in 1 M NH_4OH aqueous solution, both the bipolaron absorption and the free-carrier tailing disappear, as can be seen in Fig. 9(b).

The temperature dependence of the conductivity for PSSA-*g*-PPY, InSituComp13 and InSituComp29 are represented in Fig. 10, where the measured logarithm of conductivity is plotted against the inverse temperature 1000/*T*. As the temperature increases, the conductivity increases first and then decreases, showing a maximum at 134–142 °C. The increase in conductivity with temperature can be attributed to an increase in polaron delocalisation due to the thermal activation, whereas the decrease in conductivity at higher temperatures is due to thermal de-doping [28]. As can be seen in Fig. 10, the thermal de-doping temperature, at which the maximum conductivity is observed, shifts to higher temperature as the clay content in in situ composite increases.

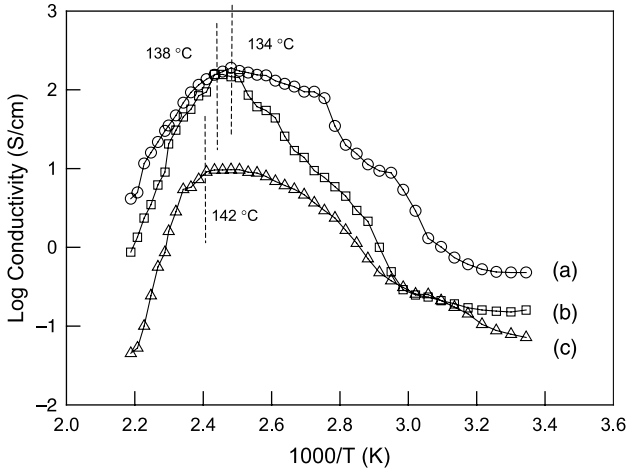

Fig. 10. The temperature dependence of the conductivity for (a) PSSA-*g*-PPY; (b) InSituComp13; (c) InSituComp29.

4. Conclusions

Exfoliated PSSA-*g*-PPY/clay nanocomposites have been successfully prepared by in situ graft polymerization of pyrrole onto pre-exfoliated P(SSA-*co*-PMS)/clay nanocomposite or by simple blending of PSSA-*g*-PPY and Na^+-MMT. SAXS, XRD patterns and TEM images clearly show exfoliation of clay layers in the polymer matrix on nanoscale. As the clay content in PSSA-*g*-PPY/clay nanocomposite increases, the logarithm of conductivity of PSSA-*g*-PPY/clay nanocomposite decreases linearly. As the clay content increases, the initiation time for graft polymerization of pyrrole decreases and the PPY content in graft copolymer increases indicating that clay catalyzes polymerization of pyrrole. Thermal de-doping temperature of PSSA-*g*-PPY in PSSA-*g*-PPY/clay nanocomposite increases as the clay content increases.

Acknowledgement

The authors thank the Korea Science and Engineering Foundation (KOSEF) for financial support through the Hyperstructured Organic Materials Research Center (HOMRC).

References

[1] Asefa T, Yoshina-Ishii C, MacLachlan MJ, Ozin GA. J Mater Chem 2000;10:1751.
[2] Boury B, Corriu RJP. Adv Mater 2000;12:989.
[3] Giannelis EP. Adv Mater 1996;8:29.
[4] Gustafasson G, Cao Y, Heeger J. Nature 1992;357:478.

[5] Skotheim TA, Elsenbaumer RL, Reynolds JF, editors. Handbook of conducting polymers. 2nd ed. New York: Marcel Dekker; 1998.
[6] Nalwa HS, editor. Handbook of organic conductive molecules and polymers. Chichester: Wiley; 1997.
[7] Wang XH, Li J, Zhang JY, Sun ZC, Yu L, Jing XB, et al. Synth Met 1999;102:1224.
[8] Biaas M, Roy AJ. Appl Polym Sci 1998;70:2169.
[9] Joo J, Lee JK, Lee SY, Jang KS, Oh EJ, Epstein AJ. Macromolecules 2000;33:5131.
[10] Kim YD, Song IC. J Mater Sci 2002;37:5051.
[11] Ruiz-Hitzky E, Aranda P, Casal B, Galván JC. Adv Mater 1995;7:180.
[12] Goren M, Qi Z, Lennox RB. Chem Mater 1995;7:171.
[13] Wong HP, Dave BC, Leroux F, Harreld J, Dunn B, Nazar LF. J Mater Chem 1998;8:1019.
[14] Peter WF, Wanli M, Alan JL, Pan W-P, Brown T. J Mater Chem 1994; 4(5):771.
[15] Faguy PW, Lucas RA, Ma WL. Colloids Surf A: Physicochem Eng Aspects 1995;105(1):105.
[16] Zeng QH, Wang DZ, Yu AB. Nanotechnology 2002;13(5):549.
[17] Orikakhi CO, Lerner MM. Mater Res Bull 1995;30(6):723.
[18] Sinharay S, Biswas M. Mater Res Bull 1999;34(8):1187.
[19] Kim JW, Liu F, Choi HJ, Hong SH, Joo J. Polymer 2003;44:289.
[20] Kim JW, Kim SG, Choi HJ, Suh MS, Shin MJ, Jhon MS. Int J Mod Phys B 2001;15:657.
[21] Kim BH, Jung JH, Hong SH, Joo JS, Epstein AJ, Mizoguchi K, et al. Macromolecules 2002;35:1419.
[22] Bae WJ, Kim KH, Park YH, Jo WH. Macromolecules 2004;37:9850.
[23] Bae WJ, Kim KH, Park YH, Jo WH. Macromolecules 2005;38:1044.
[24] Choi YS, Choi MH, Wang KH, Kim SO, Kim YK, Chung IJ. Macromolecules 2001;34:8978.
[25] Kuila BK, Nandi AK. Macromolecules 2004;37:8577.
[26] Mária O, Miroslava T, Jürgen P, Jan P, Jaroslav S. Synth Met 2004; 143:153.
[27] Rand B, Pekenc E, Goodwin JW, Smith RW. J Chem Soc, Faraday Trans 1980;76:225.
[28] Chen S-A, Hwang G-W. J Am Chem Soc 1995;117:10055.